GEOPHYSICAL RESEARCH LETTERS, VOL. 35, L17305, doi:10.1029/2008GL034903, 2008

12 May 2008 M = 7.9 Wenchuan, China, earthquake calculated to increase failure stress and seismicity rate on three major fault systems

Shinji Toda,[1] Jian Lin,[2] Mustapha Meghraoui,[3] and Ross S. Stein[4]

Received 5 June 2008; revised 16 July 2008; accepted 23 July 2008; published 9 September 2008.

[1] The Wenchuan earthquake on the Longmen Shan fault zone devastated cities of Sichuan, claiming at least 69,000 lives. We calculate that the earthquake also brought the Xianshuihe, Kunlun and Min Jiang faults 150–400 km from the mainshock rupture in the eastern Tibetan Plateau 0.2–0.5 bars closer to Coulomb failure. Because some portions of these stressed faults have not ruptured in more than a century, the earthquake could trigger or hasten additional M > 7 earthquakes, potentially subjecting regions from Kangding to Daofu and Maqin to Rangtag to strong shaking. We use the calculated stress changes and the observed background seismicity to forecast the rate and distribution of damaging shocks. The earthquake probability in the region is estimated to be 57–71% for M ≥ 6 shocks during the next decade, and 8–12% for M ≥ 7 shocks. These are up to twice the probabilities for the decade before the Wenchuan earthquake struck. **Citation:** Toda, S., J. Lin, M. Meghraoui, and R. S. Stein (2008), 12 May 2008 M = 7.9 Wenchuan, China, earthquake calculated to increase failure stress and seismicity rate on three major fault systems, *Geophys. Res. Lett.*, *35*, L17305, doi:10.1029/2008GL034903.

1. Introduction

[2] About 300 km of the Longmen Shan fault zone [*Densmore et al.*, 2007; *Burchfiel et al.*, 2008] ruptured in the Wenchan earthquake. Preliminary teleseismic waveform analysis suggests that the earthquake is composed of two sub-events of 6–9 m slip on a ~33° dipping fault; the epicentral sub-event underwent oblique right-lateral thrust slip, while the northeast sub-event slipped largely right-laterally (N. Nishimura and Y. Yagi, Rupture process for May 12, 2008 Sichuan earthquake (preliminary result), 2008, available at http://www.geol.tsukuba.ac.jp/~nisimura/20080512/ (hereinafter referred to as Nishimura and Yagi (2008)); C. Ji and G. Hayes, Preliminary result of the May 12, 2008 Mw 7.9 eastern Sichuan, China earthquake, 2008, available at http://earthquake.usgs.gov/eqcenter/eqinthenews/2008/us2008ryan/finite_fault.php (hereinafter referred to as Ji and Hayes (2008))). We use the coseismic slip to forecast how stress imparted by the earthquake may alter the distribution and rate of subsequent seismicity, potentially increasing activity on several fault systems with slip rates much higher than the Longmen Shan fault. This calculation is intended to furnish both a civic warning and a prospective test for future evaluation.

2. Coulomb Stress Changes

[3] We calculate the coseismic Coulomb stress imparted by the Wenchuan earthquake using the variable slip source models of Ji and Hayes (2008) and Nishimura and Yagi (2008) in an elastic halfspace with shear modulus of 3.2×10^5 bars. Fluid flow, inelastic behavior, and dynamic stresses are neglected. We resolve the stress changes at 10 km depth based on the estimated geometry of major active faults [*Deng et al.*, 2007; *Burchfiel et al.*, 2008], with smooth interpolation of fault geometry and rake between mapped faults (Figure 1). Increased shear stress in the rake direction and unclamping on surrounding 'receiver' faults are interpreted to promote failure. The unclamping stress depends only on the strike and dip of receiver faults; the shear stress additionally depends on their rake [*King et al.*, 1994]. The absolute level of stress is unknown, and so we can only identify faults brought closer to or farther from Coulomb failure. Nevertheless, such an approach successfully forecast the approximate location of large damaging earthquakes that struck within months of large mainshocks [*Barka*, 1999; *McCloskey et al.*, 2005].

[4] The calculated pattern of Coulomb stress changes in Figure 1 is complex, due both to the oblique coseismic slip of the Wenchuan earthquake source, and the variable strike, slip and rakes of the receiver faults. Simpler and more idealized patterns of the stress transferred by thrust and strike-slip events are given by *Lin and Stein* [2004]. In addition to stresses that promote thrust failure beyond the ends of the Longmen Shan rupture, parts of the major Xianshuihe and Kunlun left-lateral faults, and the Min Jiang reverse/left-lateral fault are brought 0.2–0.5 bars closer to failure, roughly equivalent to a decade of tectonic stress accumulation for the two major faults. In contrast, failure is inhibited by 0.1–0.3 bars on the thrust fault lying just south of Chengdu. Stress changes of ≥0.1 bars are generally observed to influence seismicity rates [*King et al.*, 1994].

[5] In Figure S1 of the auxiliary material, we perturb the calculation shown in Figure 1 for the likely range of the effective fault friction coefficent (0.0–0.8) and depth at which large earthquakes might nucleate on receiver faults (5–15 km).[1] Evident in all cases is the calculated 0.2–0.3

[1]Active Fault Research Center, Geological Survey of Japan, AIST, Tsukuba, Japan.
[2]Woods Hole Oceanographic Institution, Woods Hole, Massachusetts, USA.
[3]Institut de Physique du Globe de Strasbourg, EOST, Strasbourg, France.
[4]U.S. Geological Survey, Menlo Park, California, USA.

0094-8276/08/2008GL034903$05.00

[1]Auxiliary materials are available in the HTML. doi:10.1029/2008GL034903.

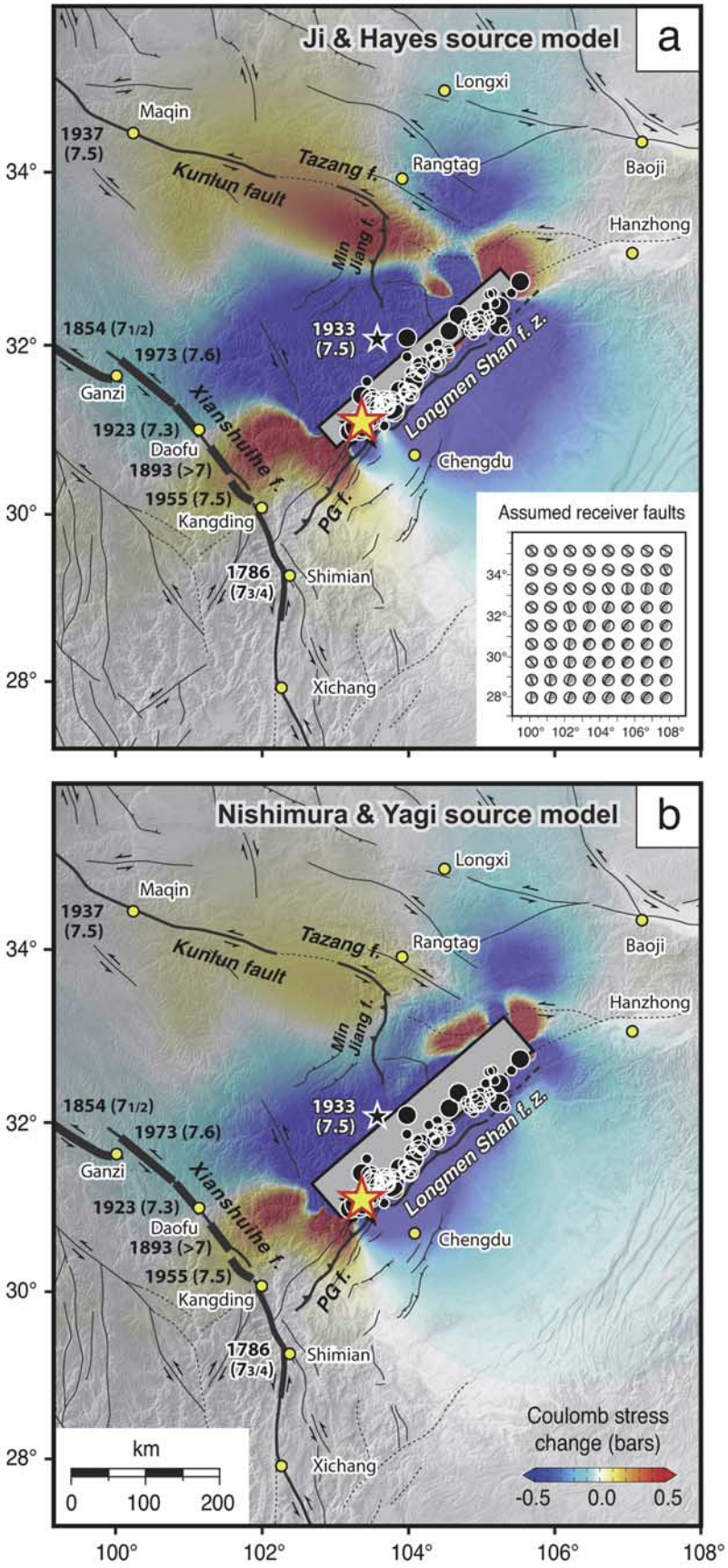
Ji & Hayes source model
a
Longxi
Maqin
1937
(7.5)
Tazang f.
Rangtag
Baoji
Kunlun fault
Min Jiang f.
Hanzhong
1854 (7 1/2)
1933
(7.5)
Longmen Shan f. z.
1973 (7.6)
Ganzi
Xianshuihe f.
1923 (7.3)
Daofu
1893 (>7)
Chengdu
1955 (7.5)
Kangding
PGT.
1786
(7 3/4)
Shimian
Xichang
Assumed receiver faults
34°
32°
30°
28°
100° 102° 104° 106° 108°
Nishimura & Yagi source model
b
Coulomb stress
change (bars)
-0.5 0.0 0.5
km
0 100 200
100° 102° 104° 106° 108°

Figure 1

bar stress increase along 250 km of the Kunlun fault system, as well as the 0.2–0.5 bar increase within the 1893 and 1955 rupture zones of the Xianshuihe fault between Daofu and Kangding. In contrast, the stress increase extending southwest of the mainshock rupture, and the increase north of Chengdu in the Sichuan basin, are sensitive to friction because of their location. Faults with large cumulative slip such as the Xianshuihe and Kunlun tend to be smoother [*Parsons et al.*, 1999], and so we suspect that friction is low on these faults (0.2–0.4) and high on the Longmen Shan and Pengguan (0.6–0.8), with slip rates of ~1 mm/yr [*Burchfiel et al.*, 2008]. Coulomb methods and uncertainties are treated more fully in the auxiliary material.

3. Large Earthquake Occurrence

[6] Large historic shocks have struck portions of the stressed faults, and for some sections a significant slip deficit has since accumulated. The Xianshuihe fault between Daofu and Kangding last ruptured in M > 7 earthquakes in 1893 and 1955 [*Allen et al.*, 1991] (Figure 1). Although large earthquakes struck the western (87°–98°E) Kunlun fault in 1937 (Ms = 7.5), 1997 (Mw = 7.6), and 2001 (Mw = 7.8) [*Lin et al.*, 2006], the eastern Kunlun and Tazang fault have suffered no known historic ruptures [*Lin et al.*, 2006; *Kirby et al.*, 2007]. The southern end or extension of the Min Jiang fault ruptured in a M~7.5 event in 1933 [*Chen et al.*, 1994]. A rough indication of the maximum size of potential earthquakes on these fault systems can be gaged by the length of the gap between recent earthquakes (Table 1, first to third columns). Given the estimated fault slip rates and the time since the last known event on these faults, we also estimate a slip deficit, which ranges between 1–10 m (Table 1, seventh column). In most cases the slip deficit exceeds the mean slip expected for the maximum earthquakes. Thus, large earthquakes are possible on several major fault systems regardless of the stress contributed by the Wenchuan earthquake.

[7] Several of the fault segments brought closer to Coulomb failure have accumulated large slip deficits. Given a slip rate of 11–15 mm/yr on the Xianshuihe fault [*Allen et al.*, 1991; *Thatcher*, 2007] and assuming a fault width of 15 km, a slip deficit equal to a Mw = 7.0 earthquake has accumulated at the site of the 1893 event in the intervening 115 years, posing a threat to Kangding, Daofu, and surrounding towns (Table 1). Some 300 km of the eastern Kunlun fault east of Maqin, with a 6–16 mm/yr slip rate [*Thatcher*, 2007; *Lin et al.*, 2006; *Kirby et al.*, 2007], is calculated to have been brought 0.2–0.3 bars closer to failure by the 12 May event. Large triggered earthquakes on the eastern Kunlun fault could expose towns between Maqin and Rangtag and adjacent areas to strong shaking. The northern part of the Min Jiang fault was also brought 0.3–0.4 bars closer to thrust failure.

4. Expected Seismicity Rate Change

[8] To forecast the impact of the stress changes on seismicity, we apply rate/state friction of *Dieterich* [1994] in a manner following *Toda et al.* [2005]. Here, a sudden stress increase causes a sudden jump in seismicity rate that decays inversely with time and eventually recovers, the duration of the transient inversely proportional to the fault stressing rate. In addition, the higher the rate of seismicity at the time of a stress increase, the more strongly the seismicity rate will be amplified by a stress increase. This means that sites or faults with a high rate of seismicity before the mainshock will be most responsive to the stress change, whereas sites with low or no seismicity will undergo little or no response. Because these effects are transient, the impact of all but the largest stress change disappears in several decades to centuries.

[9] To calculate the expected seismicity rate, we need the reference or background seismicity rate before the mainshock. We must also assume a value of $A\sigma$, where A is a rate/state constitutive parameter and σ is the total normal stress. Experimental and observational values of $A\sigma$ are uncertain, with 0.1–0.5 bars most commonly applied [e.g., *Toda et al.*, 2005; *Catalli et al.*, 2008]. We also require a duration for the transient effect, roughly equivalent to the aftershock duration, t_a, the time needed for the aftershock rate to recover to the pre-mainshock seismicity rate. Since t_a is thought to be 5–10% of an interseismic cycle [*Dieterich*, 1994], we assume the range of t_a is 10–100 yr in the study area, consistent with California t_a measurements [*Toda et al.*, 2005] and with likely interevent times on the Sichuan faults [*Burchfiel et al.*, 2008]. These methods are treated more fully in the auxiliary material. To maximize the number of earthquakes used to infer the reference seismicity rate, we calculate the magnitude of completeness for the Wenchuan area from the ISC catalog (Figure 2a inset), and use M $\geq$ 3.2 shocks during 2000–2008, smoothed with a 50-km radius cylinder (Figures 2a and 2b). A realization of the expected seismicity rates during the decade, 2008–2017, using the Ji and Hayes (2008) source model is shown in Figure 2c; the range of forecast seismicity rates on key fault patches for a broad range of parameters is given in Table 2 and Figure S2.

[10] Areas redder in Figure 2c than in Figure 2b are forecast to undergo seismicity rate gains resulting from the Coulomb stress increase. By assuming a magnitude-frequency b-value of 1.0, the overall probability of a M > 6 shock striking somewhere in the 750 × 780 km area is estimated to be 47–71% during the next decade, compared with 49% for the

Figure 1. Coulomb stress calculated at 10 km depth assuming an apparent fault friction of 0.4, using the (a) Ji and Hayes (2008) and (b) Nishimura and Yagi (2008) earthquake source models. Yellow star and black dots indicate mainshock and 12–20 May 2008 aftershocks. Historical ruptures on Xianshuihe fault are marked by the thickest black lines [*Allen et al.*, 1991], mapped faults are thick black lines, faults active in the past 10 Ky are thin black lines, those active in the past 1 My are dashed [*Densmore et al.*, 2007; *Kirby et al.*, 2007; *Deng et al.*, 2007]. PG f., Pengguan fault. Stresses are resolved on the faults on each region with smooth interpolation between mapped faults; the inset box gives the matrix of assumed receiver fault focal mechanisms (lower hemisphere projection) with the selected fault plane inscribed in black. This is a departure from typical Coulomb plots in which either one fault orientation is assumed for the entire area, or stress changes are resolved only on selected faults. Calculations used Coulomb 3.1 (http://www.coulombstress.org).

Table 1. Estimated Slip Deficit on Major Active Faults

Fault Segment[a]	Notation	Gap Length (km)	Equivalent Mw[b]	Slip Rate (mm/yr)	Time Since Most Recent Earthquake (y.B.P.)	Resulting Slip Deficit (m)
Eastern Kunlun	K	260	7.9	2–12	>1800	>3.6–21.6
Tazang	T	35–55	6.6–6.9	<1	>9000	<9
Min Jiang	M	100	7.5	<1	>7000	<7
Pengguan NW segment	P	110–120	7.5–7.6	-	-	-
Xianshuihe 1893 segment	X1	65	7.0	15 ± 5	115	1.2–2.3
Xianshuihe 1786 segment	X2	135	7.5	5	222	1.1

[a]Shown in Figure 2c.
[b]Mw is calculated from empirical relations between subsurface fault length and Mw based on *Wells and Coppersmith* [1994].

Table 2. Coulomb Stress and Seismicity Rate Changes on Major Active Faults

Fault Segment[a]	Notation	Dip (deg)	Rake (deg)	References[b]	Max ΔCFF[c] (Bars)	Seismicity Rate Change[d] (R/r)
Eastern Kunlun	K	90	0	1, 2, 3	0.07	1.1–1.9
Tazang	T	90	0	3	0.23	1.3–7.5
Min Jiang	M	45–65	45–135	4	0.33	1.5–13.5
Pengguan NW Segment	P	25–45	90–135	5	4.19	8.9–118.9
Xianshuihe 1893 Segment	X1	90	0	6	0.19	1.3–5.3
Xianshuihe 1786 Segment	X2	90	0	6	0.04	1.1–1.5

[a]Shown in Figure 2c.
[b]1) *Van der Woerd et al.* [2002]; 2) *He et al.* [2006]; 3) *Kirby et al.* [2007]; 4) *Kirby et al.* [2000]; 5) *Densmore et al.* [2007]; and 6) *Allen et al.* [1991].
[c]Max ΔCFF represents the maximum Coulomb stress changes resolved on the indicated fault at depths of 10–15 km with apparent coefficient of friction 0.0–0.8.
[d]Seismicity rate change is a ratio of expected seismicity rate after the Wenchuan mainshock (R) to the rate before the mainshock (r) during 10 yr. To calculate R in the rate- and state-friction framework, we used t_a = 10–100 years, and Aσ = 0.1–0.5 bar.

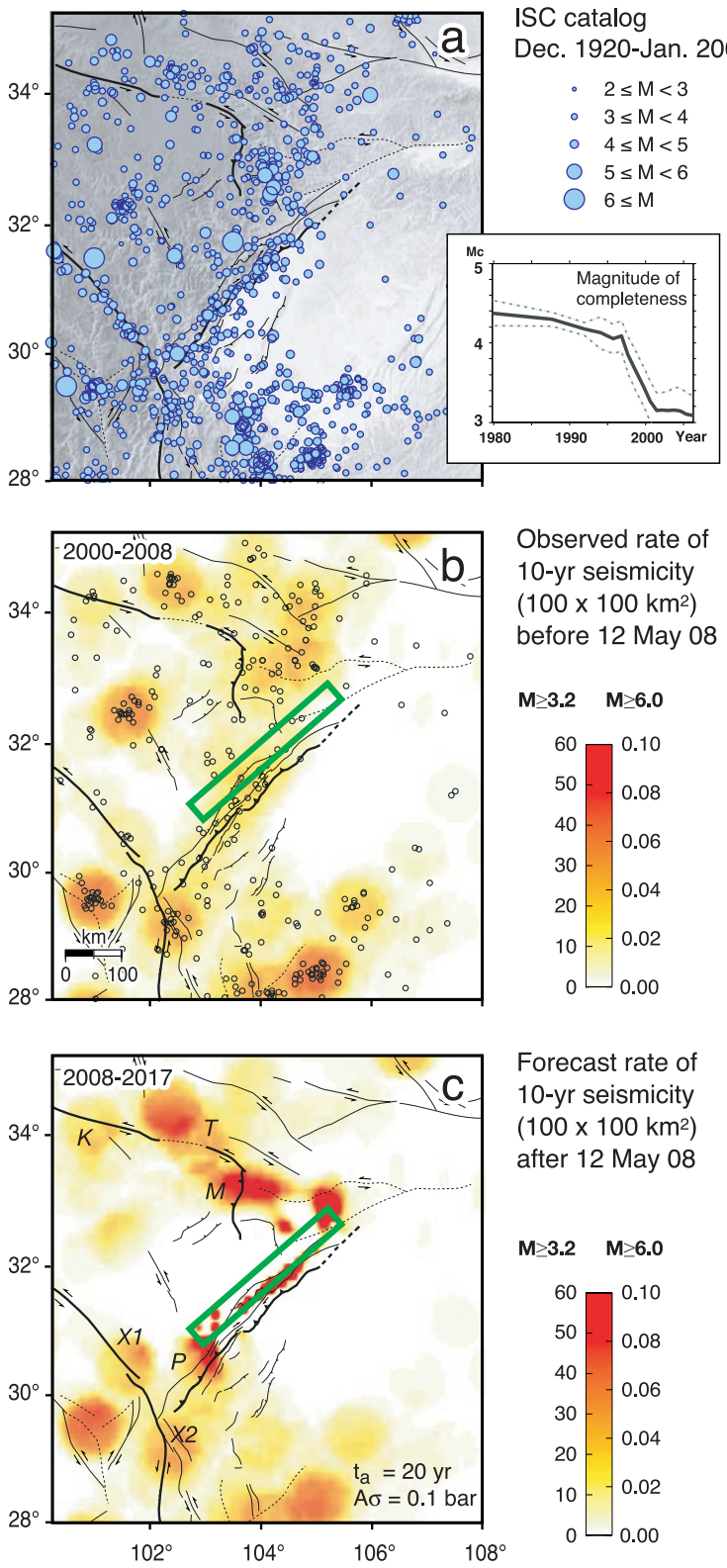

Figure 2. Forecast of the next decade of earthquakes based on preceding seismicity and the Coulomb stress imparted by the Wenchuan rupture. (a) The ISC catalog was smoothed with a 50 km-radius Gaussian filter for the period 2000–2008 to estimate the distribution of (b) seismicity rate before the Wenchuan mainshock. Coulomb stress increases amplify the (c) seismicity rates in areas of high backgound rate, so that areas redder in Figure 2c than in Figure 2b are forecast to undergo seismicity rate gains. These include K, Kunlun; T, Tazang; M, Min Jiang; X1 and X2, Xianshuihe 1893 and 1786 rupture segments; and P, Pengguan (sites keyed to Table 2). In constrast, areas in stress shadows in Figure 1 are whiter in Figure 2c than Figure 2b. By assuming a magnitude-frequency b-value of 1.0, we also show the expected rate of M $\geq$ 6 shocks in Figure 2c.

preceding decade. The probability of a M $\geq$ 7 shock is 6–12%, compared with 7% during the preceding decade; the range reflects the full parameter variation in Table 2 and Figure S2. The lower probability bound corresponds to t_a = 10 yr, which is applicable only to the most active faults. For the region as a whole, we regard the 100-yr t_a value as more appropriate, which results in a M $\geq$ 7 forecast for the next decade of 8–12%, or 23–31% for the next 30 years. The forecast seismicity rate increases on the Min Jiang fault and along the 1893 rupture zone of the Xianshuihe fault (M and X1, respectively, in Figure 2c and Table 2) coincide with large slip deficits, and so would seem to be particularly vulnerable to subsequent earthquakes.

5. Conclusions

[11] The forecast rate of M $\geq$ 3.2 shocks for the next decade (Figure 2c) provides a testable hypothesis for the future distribution and rate of earthquakes that can be compared to the preceding rate (Figure 2b) as a control population. If an increased rate of such small shocks is observed on the stressed parts of the Xianshuihe, Kunlun, and Min Jiang faults, it would provide support for the hypothesis that large shocks are now also more likely where the static stress imparted by the mainshock has risen. The M $\geq$ 6 and M $\geq$ 7 forecasts are offered as an index of seismic hazard, since earthquakes of this size can be highly damaging. The Wenchuan earthquake thus poses a continuing seismic hazard, and also provides a test of earthquake promotion.

[12] **Acknowledgments.** We thank M. Blanpied, W. Thatcher, R. Harris, and G. Fuis for reviews. S. T. and R. S. are grateful for research fellowships at EOST- Institut de Physique du Globe de Strasbourg, France. J. L. was supported by the Charles D. Hollister Endowed Fund for Support of Innovative Research at WHOI.

References

Allen, C. R., Z. Luo, H. Qian, X. Wen, H. Zhou, and W. Huang (1991), Field study of a highly active fault zone: The Xianshuihe fault of southwestern China, *Geol. Soc. Am. Bull.*, *103*, 1178–1199.

Barka, A. (1999), The 17 August 1999 Izmit earthquake, *Science*, *285*, 1858–1859.

Burchfiel, B. C., et al. (2008), A geological and geophysical context for the Wenchuan earthquake of 12 May 2008, Sichuan, People's Republic of China, *GSA Today*, *18*, 4–11, doi:10.1130/GSATG18A.1.

Catalli, F., M. Cocco, R. Console, and L. Chiaraluce (2008), Modeling seismicity rate changes during the 1997 Umbria-Marche sequence (central Italy) through a rate- and state-dependent model, *J. Geophys. Res.*, doi:10.1029/2007JB005356, in press.

Chen, S. F., C. J. L. Wilson, Q. D. Deng, X. L. Zhao, and Z. L. Luo (1994), Active faulting and block movement associated with large earthquakes in the Min Shan and Longmen Mountains, northeastern Tibetan Plateau, *J. Geophys. Res.*, *99*, 24,025–24,038.

Deng, Q.-D., et al. (2007), Active tectonics map of China, Earthquake Press, Beijing.

Densmore, A. L., M. A. Ellis, Y. Li, R. Zhou, G. S. Hancock, and N. Richardson (2007), Active tectonics of the Beichuan and Pengguan faults at the eastern margin of the Tibetan Plateau, *Tectonics*, *26*, TC4005, doi:10.1029/2006TC001987.

Dieterich, J. (1994), A constitutive law for rate of earthquake production and its application to earthquake clustering, *J. Geophys. Res.*, *99*, 2601–2618.

He, W., Z. Xiong, D. Yuan, W. Ge, and X. Liu (2006), A preliminary study of paleo-earthquakes on the Maqu fault of the East Kunlun fault zone, *Earthquake Res. China*, *20*, 361–370.

King, G. C. P., R. S. Stein, and J. Lin (1994), Static stress changes and the triggering of earthquakes, *Bull. Seismol. Soc. Am.*, *84*, 935–953.

Kirby, E., K. X. Whipple, B. C. Burchfiel, W. Tang, G. Berger, Z. Sun, and Z. Chen (2000), Neotectonics of the Min Shan, China: Implications for mechanisms driving Quaternary deformation along the eastern margin of the Tibetan Plateau, *Geol. Soc. Am. Bull.*, *112*, 375–393.

Kirby, E., N. Harkins, E. Wang, X. Shi, C. Fan, and D. Burbank (2007), Slip rate gradients along the eastern Kunlun fault, *Tectonics*, *26*, TC2010, doi:10.1029/2006TC002033.

Lin, A., B. Fu, J. Guo, Q. Zeng, G. Dang, W. He, and Y. Zhao (2002), Co-seismic strike-slip and rupture length produced by the 2001 M_s 8.1 central Kunlun earthquake, *Science*, *296*, 2015–2017.

Lin, A., J. Guo, K. Kano, and Y. Awata (2006), Average slip rate and recurrence interval of large-magnitude earthquakes on the western segment of the strike-slip Kunlun fault, northern Tibet, *Bull. Seismol. Soc. Am.*, *96*, 1597–1611.

Lin, J., and R. S. Stein (2004), Stress triggering in thrust and subduction earthquakes and stress interaction between the southern San Andreas and nearby thrust and strike-slip faults, *J. Geophys. Res.*, *109*, B02303, doi:10.1029/2003JB002607.

McCloskey, J., S. S. Nalbant, and S. Steacy (2005), Earthquake risk from co-seismic stress, *Nature*, *434*, 291.

Parsons, T., R. S. Stein, R. W. Simpson, and P. A. Reasenberg (1999), Stress sensitivity of fault seismicity: A comparison between limited-offset oblique and major strike-slip faults, *J. Geophys. Res.*, *104*, 20,183–20,202.

Thatcher, W. (2007), Microplate model for the present-day deformation of Tibet, *J. Geophys. Res.*, *112*, B01401, doi:10.1029/2005JB004244.

Toda, S., R. S. Stein, K. Richards-Dinger, and S. B. Bozkurt (2005), Forecasting the evolution of seismicity in southern California: Animations built on earthquake stress transfer, *J. Geophys. Res.*, *110*, B05S16, doi:10.1029/2004JB003415.

Van der Woerd, J., P. Tapponnier, F. J. Ryerson, A.-S. Meriaux, B. Meyer, Y. Gaudemer, R. C. Finkel, M. W. Caffee, G. Zhao, and Z. Xu (2002), Uniform postglacial slip-rate along the central 600 km of the Kunlun Fault (Tibet), from ^{26}Al, ^{10}Be, and ^{14}C dating of riser offsets, and climatic origin of the regional morphology, *Geophys. J. Int.*, *148*, 356–388.

Wells, D. L., and K. J. Coppersmith (1994), New empirical relationships among magnitude, rupture length, rupture width, rupture area, and surface displacement, *Bull. Seismol. Soc. Am.*, *84*, 974–1002.

J. Lin, Woods Hole Oceanographic Institution, 266 Woods Hole Road, Woods Hole, MA 02543, USA.

M. Meghraoui, Institut de Physique du Globe de Strasbourg, EOST, 5, rue Rene Descartes, F-67084 Strasbourg CEDEX, France.

R. S. Stein, U.S. Geological Survey, 345 Middlefield Road, Menlo Park, CA 94025, USA.

S. Toda, Active Fault Research Center, Geological Survey of Japan, AIST, Site 7, Higashi 1-1, Tsukuba 305-8567, Japan. (s-toda@aist.go.jp)